LETTER

doi:10.1038/nature10589

Frictional ageing from interfacial bonding and the origins of rate and state friction

Qunyang Li[1]†, Terry E. Tullis[2], David Goldsby[2] & Robert W. Carpick[1]

Earthquakes have long been recognized as being the result of stick–slip frictional instabilities[1,2]. Over the past few decades, laboratory studies of rock friction have elucidated many aspects of tectonic fault zone processes and earthquake phenomena[3–5]. Typically, the static friction of rocks grows logarithmically with time when they are held in stationary contact[6], but the mechanism responsible for this strengthening is not understood. This time-dependent increase of frictional strength, or frictional ageing, is one manifestation of the 'evolution effect' in rate and state friction theory[5]. A prevailing view is that the time dependence of rock friction results from increases in contact area caused by creep of contacting asperities[7,8]. Here we present the results of atomic force microscopy experiments that instead show that frictional ageing arises from the formation of interfacial chemical bonds, and the large magnitude of ageing at the nanometre scale is quantitatively consistent with what is required to explain observations in macroscopic rock friction experiments. The relative magnitude of the evolution effect compared with that of the 'direct effect'—the dependence of friction on instantaneous changes in slip velocity—determine whether unstable slip, leading to earthquakes, is possible[9,10]. Understanding the mechanism underlying the evolution effect would enable us to formulate physically based frictional constitutive laws, rather than the current empirically based 'laws'[11,12], allowing more confident extrapolation to natural faults.

Frictional ageing has been attributed to increases in contact area caused by asperity creep (contact 'quantity') as well as to time-dependent strengthening of bonding at asperity contacts (contact 'quality'). Evidence exists to support both interpretations. By measuring the amount of light transmitted across rough Lucite plastic surfaces in contact, and rough soda-lime glass surfaces in contact, Dieterich and Kilgore[8] observed gradual increases in the sizes of illuminated microscopic contacts over time. Experiments on a silicate rock (quartzite) have demonstrated that frictional ageing is suppressed by drying the samples and conducting friction experiments in a water-free environment[7]. Because creep is inhibited in experiments on silicate minerals like quartz at high temperature in the absence of water (that is, in the absence of hydrolytic weakening[13]), these observations are consistent with the hypothesis that static friction increases with changes in contact area caused by asperity creep[14]. However, frictional ageing may also result from strengthening of chemical bonding at the interface over time. Chemical bonding could be enhanced by time-dependent desorption of contamination films[15] that may include water, or through chemically assisted mechanisms (such as hydrogen bonding or siloxane bridging)[16–18] that can be aided by water and also affected by the contact stresses.

Devising experiments to understand the contribution of each mechanism to ageing is exceedingly difficult, because the buried frictional interface is not readily accessible and involves myriad microscopic asperity contacts with a range of sizes down to the nanoscale[19,20]. Here, we investigate the ageing behaviour of a single nanoscale contact to isolate the physical origins of the ageing process and provide new perspectives on the empirical rate- and state-dependent friction laws.

We conducted single-asperity slide–hold–slide (SA-SHS) friction experiments between nanoscopically sharp oxidized silicon tips and oxidized silicon wafers using an atomic force microscope (AFM); these tests are analogous to similar slide–hold–slide tests on rocks[3,6]. The use of amorphous SiO_2 (silica) to investigate the behaviour of rocks composed of silicate minerals is reasonable, because silica glass and rocks behave similarly in friction experiments on rough surfaces[21].

Figure 1 shows an example of SA-SHS measurements performed at 60% relative humidity (RH). Similar to slide–hold–slide experiments on rocks[3,6], the static friction force is larger than the steady-state sliding friction force by an amount ΔF, called the friction drop, that grows linearly with the logarithm of the hold time (inset to Fig. 1). Similar trends are obtained at other humidities. The linear dependence of ΔF on the logarithm of hold time is consistent with observations from friction experiments on macroscopic rocks and other materials[6,16], but the magnitude observed here is far larger. The ratio between ΔF and the steady-state friction F_{ss} ($\Delta F/F_{ss}$), which we call the 'relative friction drop', ranges from 0.5 to 5 over the range of humidity studied for 100-s hold times, compared to less than 0.05 for a 100-s hold time observed for macroscopic quartz rock samples[16]. This unusually large ageing effect is reproducible for all the SA-SHS experiments, with more than five distinct silica–silica pairs tested.

The much larger ageing of the relative friction drop at the nanoscale than at the macroscale suggests that frictional ageing may be a length-scale-dependent phenomenon influenced by the multi-asperity

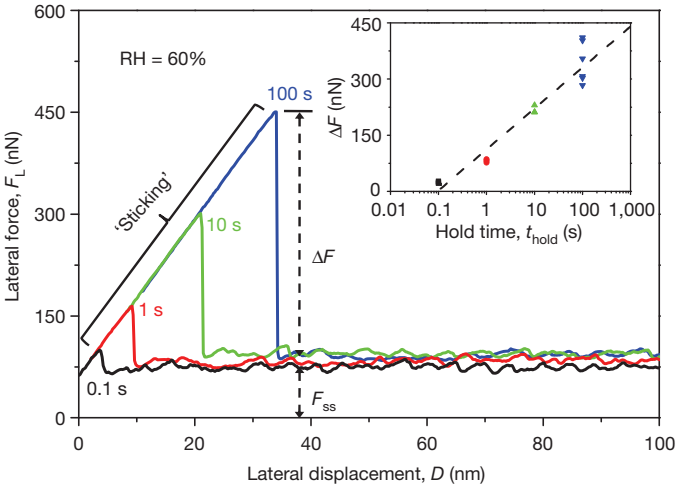

Figure 1 | Lateral force versus nominal lateral displacement data for typical SA-SHS tests after stationary holds at 60% RH. Upon lateral displacement, the tip sticks to the substrate, resulting in linear, elastic lateral loading of the AFM cantilever (Supplementary Figs 1 and 2). When the lateral force exceeds static friction, the tip slips forward, indicated by abrupt drops in lateral force (ΔF), followed by subsequent sliding at the steady-state friction force (F_{ss}). In the inset ΔF varies linearly with the logarithm of hold time. The dotted line is a linear fit of the averaged values.

[1]Department of Mechanical Engineering and Applied Mechanics, University of Pennsylvania, Philadelphia, Pennsylvania 19104, USA. [2]Department of Geological Sciences, Brown University, Providence, Rhode Island 02912, USA. †Present address: School of Aerospace, Tsinghua University, Beijing 100084, China.

character of rough surfaces. To test this hypothesis, we construct a simplified mechanics model to predict friction as a function of nominal contact size for a fixed number of discrete asperities per unit area (Fig. 2). Comparing a small (19 asperities) and large (1,459 asperities) nominal contact area, with the same individual asperity (i) relative friction drop ($\Delta F^i/F^i_{ss}=1$), the total macroscopic relative friction drop ($\Delta F^{total}/F^{total}_{ss}$) values are very different: 0.81 for the smaller nominal contact and 0.15 for the larger nominal contact. The behaviour can be understood as follows. Owing to elastic interactions between asperities through the substrate, the asperities do not experience the same shear stress and thus do not slide simultaneously; the shear stress rises from the contact centre outward, until slip occurs. For sufficiently small nominal contact areas, asperities slide nearly at the same time, so macroscopic ageing is similar to individual asperity ageing. However, for larger nominal contacts, only a small fraction of asperities experience the peak forces at any given time: those in the outermost annulus have slid and thus relaxed the peak stress to the much lower steady-state sliding value, thus providing little extra resistance, whereas those in the centre have not yet been stressed to the peak shear stress, thus providing little contribution to the measured friction force. Therefore, only a small internal annulus of asperities exhibit the peak shear stress, and hence $\Delta F^{total}/F^{total}_{ss}$ of a nominally micrometre-sized contact interface that has nanoscale asperities will be less than 10% of the corresponding values for the single asperities.

Although the model is highly idealized, it demonstrates a general behaviour: larger nominal contacts will generally have a much lower macroscopic ageing effect than that measured for individual asperities within the nominal contact area regardless of the specific mechanism(s) for ageing. This can account for the different magnitudes of frictional ageing seen in rock friction experiments on rough surfaces[6,16] and in the single-asperity experiments. This scale dependence is somewhat analogous to that observed for adhesion: small objects adhere to surfaces far more strongly (relative to their weight) than macroscopic objects, owing to the numerous asperities on rough surfaces of large objects[22].

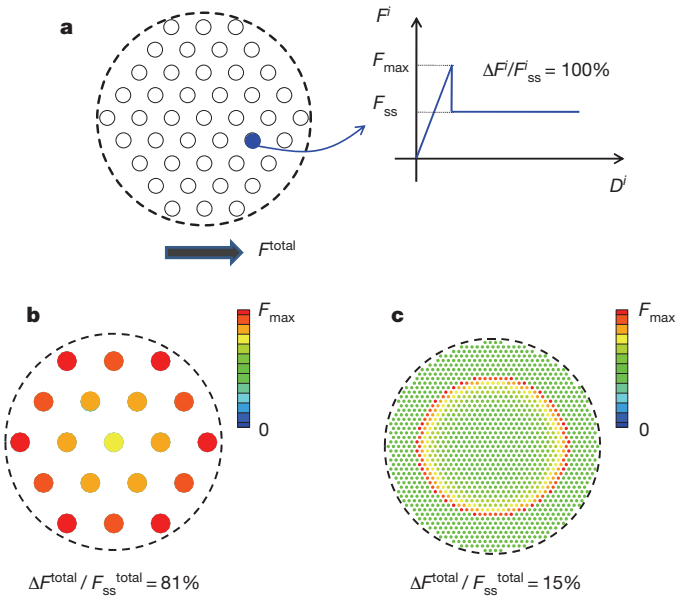

Figure 2 | The quasi-static discrete asperity model. a, An interface between a rigid top surface and an elastic half space with a circular nominal contact area encompassing identical close-packed circular asperities at fixed spacing (small circles), all with maximum static friction force F_{max} (with $\Delta F^i/F^i_{ss}=1$). Upon lateral loading by F^{total}, asperities are uniformly elastically strained up to their maximum static friction, whereupon they slip (see Supplementary Information). The shear force distributions at the peak frictional force for 19 (**b**) and 1,459 (**c**) asperities result in macroscopic relative static friction ($\Delta F^{total}/F^{total}_{ss}$) that is high (0.81) for **a** but much lower (0.15) for **c**.

Although the unusually large ageing effect at the single-asperity level revealed by our experiments is required to explain the frictional ageing observed in friction experiments on rough macroscopic rock surfaces, the results presented thus far do not identify the underlying cause of this large ageing effect. In the present SA-SHS experiments, we found that ageing can depend critically on the chemical state of the AFM tip (Fig. 3). We found that frictional ageing was substantially but reversibly suppressed when the AFM tip was pulled out of contact and exposed to the humid environment before undergoing an SA-SHS test; ageing could be revitalized by sliding the tip across the substrate for some cumulative run-in sliding distance (and by not breaking contact immediately before an SA-SHS test). While the tip is out of contact, the tip is susceptible to adsorption of gaseous species, including organics (well known to reduce the surface energy of silica surfaces)[23], whereas during scanning of the tip on the substrate, such adsorption is suppressed and adsorbates can be removed. This clearly indicates that plastic deformation of the tip is not involved in the frictional ageing observed in the SA-SHS tests, given that lifting up and sliding the tip would not influence plastic deformation of the tip in such a reversible manner.

The surfaces of oxidized silicon samples cleaned with Piranha solution (5:1 concentrated sulphuric acid to 30% hydrogen peroxide solution) are highly hydroxylated[24,25]. In a humid environment, hydrogen bonding can arise between two hydroxylated silica surfaces[17,18,25], which, together with van der Waals and capillary interactions, will increase the overall interfacial adhesion and friction. Furthermore, at raised temperatures the silanol (Si–OH) groups from opposing sides of contacting surfaces can react to form stronger siloxane (Si–O–Si) bonds[17,25]. At room temperature (typically 23 °C), with applied load and sufficient time, the reaction may also proceed[17], but the kinetics have yet to be studied in detail. Capillary interactions are unlikely to be a dominant mechanism because of the persistence of ageing at humidities below 1% RH (see Supplementary Fig. 5). Therefore, we hypothesize that frictional ageing is caused by hydrogen or siloxane bond formation across the interface.

To test this hypothesis, we performed another set of SA-SHS tests by sliding a silica tip over two chemically inert surfaces: hydrogen-terminated diamond, and graphite. The diamond sample is grown by chemical vapour deposition (typical grain size ~1 μm) and subsequently exposed to atomic hydrogen using an established method[26] that produces a highly uniform, nearly oxygen-free, monohydride surface before the friction experiment. The graphite surface was prepared by freshly cleaving a bulk highly ordered pyrolytic graphite sample. Interfacial bonding is not expected between silica and either

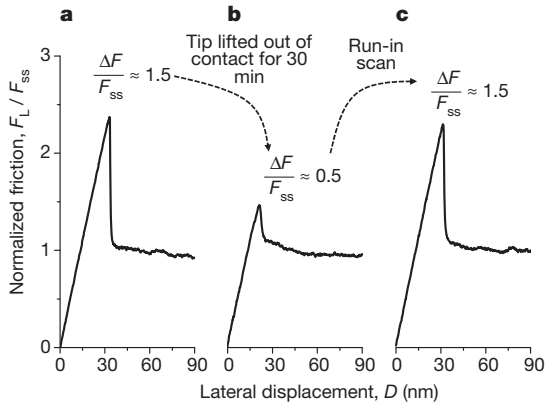

Figure 3 | Normalized friction–displacement curves from three sequential SA-SHS tests. a, Typical, strong ageing is seen immediately after a first run-in scan (cumulative displacement of ~1 mm); $\Delta F/F_{ss}=1.5$. **b**, Ageing is substantially suppressed after 30 min of exposure of the tip to the humid environment, out of contact with the sample, followed immediately by the SA-SHS test shown; $\Delta F/F_{ss}=0.5$. **c**, Large ageing returned to the original value after sliding for another run-in scan; $\Delta F/F_{ss}=1.5$. All tests used a 100-s hold time at 40% RH, with a negative lateral hold force (see Supplementary Information).

H-terminated diamond or graphite. The normalized friction versus displacement plots from SA-SHS tests (100-s hold time) are shown in Fig. 4 and compared with data from the oxidized silicon surface. In contrast to the significant frictional ageing (static friction increases by a factor of six compared to the steady-state friction) for the silica–silica surface, the silica–diamond interface and the silica–graphite interface show little to no ageing. Contact stresses are estimated to be about 0.2 GPa, 0.4 GPa and 1.5 GPa for silica–silica, silica–graphite and silica–diamond contacts respectively (see Supplementary Fig. 8). If plastic creep occurs for the silica–silica contact, we would also expect it in the tip for all of the systems, leading to a similarly high degree of ageing (perhaps even more for the silica–diamond contact where the contact stresses were largest). However, given the indentation hardness of amorphous silica of approximately 12 GPa (ref. 27), we would not expect plastic creep in the tip for any of these material pairs at the normal stresses involved. Given both this expectation and the results shown in Figs 1, 3 and 4, our experiments clearly demonstrate that the frictional ageing effect in SA-SHS tests does not primarily arise from plastic creep, but from changes in bonding arising from surface chemical processes.

In conclusion, we find that frictional strength for AFM tips of silica sliding on a silica substrate increases linearly as a function of the logarithm of contact time, in the same fashion as the frictional strengths of silicate minerals in macroscopic friction experiments. However, the magnitude of the ageing effect for the nanoscale single-asperity contacts is much larger than for macroscopic multi-asperity rock friction experiments. We demonstrate that this difference should be expected given the scales and single- versus multi-asperity geometries of the two cases regardless of the specific mechanisms for ageing. At the nanometre scale and at relatively low contact stresses, frictional ageing cannot be explained by increases in contact area due to plastic creep. Rather, it is associated with changes in chemical bonding as demonstrated by the dependence of ageing on the identity of the samples that are in contact with the AFM tips, and the reversible suppression of ageing by removing the tip from otherwise continuous contact with the sample. This reduction of ageing due to exposure of the interface to ambient conditions may contribute partially to the low frictional ageing observed in macroscopic rock friction experiments. In such experiments, both contacting surfaces are usually rough and the local asperities can be exposed to water or other contaminants intermittently during sliding. However, this effect alone is insufficient to account for the very large difference in ageing we observe; variations in relative frictional ageing before and after breaking the contact within our experiment is typically between 0.5–5, whereas the difference between our results and macroscopic experiments is two orders of magnitude.

The magnitude of ageing from these chemical-bonding effects is large enough to account for the evolution effect in rate and state friction without a time-dependent increase in contact area. Whether the primary cause of frictional ageing in macroscopic friction experiments is an increase in the quantity and strength of chemical bonding or an increase in contact area due to plastic creep is unresolved by our data. However, we have demonstrated that chemical bonding is a viable explanation, although we have not determined the specific chemical mechanism that leads to such a slow, logarithmic ageing. The logarithmic behaviour demonstrates that the rate of reaction is slowing down as a function of time. Further experimental and theoretical studies are needed to address the mechanism(s) that account for this.

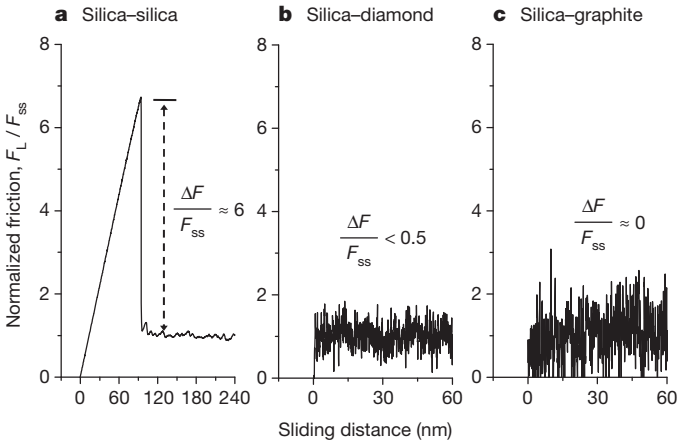

Figure 4 | Three SA-SHS tests between a silica tip and three different surfaces. **a**, Silica–silica; **b**, silica–hydrogen-terminated diamond; **c**, silica–graphite. The tests were all performed at 60% RH for a 100-s hold time. The normal load in each case is maintained at approximately 1 nN. The lateral forces during stationary hold are negative (see Supplementary Information).

METHODS SUMMARY

Experiments were conducted by sliding silica AFM tips over silica surfaces using friction force microscopy (see Methods and Supplementary Fig. 1). The probes and substrate are processed by heating silicon probes and Si(100) wafers in pure oxygen to form oxides 100 nm and 400 nm thick respectively. The substrates were cleaned with Piranha solution, rinsed with de-ionized water, dried under pure nitrogen flow, then rapidly inserted into the AFM. The substrates have a typical root-mean-square roughness of ~0.2 nm within a 0.5 μm × 0.5 μm area, according to the AFM. Normal and lateral force constants of the probes were calibrated using Sader's method[28] and a diamagnetic lateral force calibrator[29] respectively. All measurements are carried out in a sealed chamber with RH varied from <1% to 80%. The system was equilibrated for at least 4 h after each humidity change to reduce thermal positional drift, which is particularly important when long hold times are used. The remaining drift may contribute to the increased scatter seen at longer hold times. This increased scatter may also be due to higher sensitivity of the interfacial strength to any inhomogeneities at the interface. RH was monitored by a hygrometer (uncertainty ±1.5% RH). A typical friction experiment is performed by first making contact between the tip and substrate, then sliding for an initial run-in distance. Then, without breaking contact, a slide–hold–slide procedure is used in which the tip is slid for a prescribed distance (typically ~400 nm), then held stationary for a time t_{hold}, and then lateral displacement is resumed. Constant normal load is imposed by a feedback loop. Four different hold times, in an alternating sequence of 0.1 s, 100 s, 1 s and 10 s, are used. The lateral force during the stationary hold was maintained at either a positive or negative value (see Methods, Supplementary Figs 2, 6 and 7 and associated discussion).

Full Methods and any associated references are available in the online version of the paper at www.nature.com/nature.

Received 9 May; accepted 21 September 2011.
Published online 30 November 2011.

1. Brace, W. F. & Byerlee, J. D. Stick-slip as a mechanism for earthquakes. *Science* **153,** 990–992 (1966).
2. Scholz, C. H. Earthquakes and friction laws. *Nature* **391,** 37–42 (1998).
3. Marone, C. Laboratory-derived friction laws and their application to seismic faulting. *Annu. Rev. Earth Planet. Sci.* **26,** 643–696 (1998).
4. Scholz, C. H. *The Mechanics of Earthquakes and Faulting* 2nd edn (Cambridge University Press, 2002).
5. Tullis, T. E. Rock friction constitutive behavior from laboratory experiments and its implications for an earthquake prediction field monitoring program. *Pure Appl. Geophys.* **126,** 555–588 (1988).
6. Dieterich, J. H. Time-dependent friction in rocks. *J. Geophys. Res.* **77,** 3690–3697 (1972).
7. Dieterich, J. H. & Conrad, G. Effect of humidity on time-dependent and velocity-dependent friction in rocks. *J. Geophys. Res.* **89** (B6), 4196–4202 (1984).
8. Dieterich, J. H. & Kilgore, B. D. Direct observation of frictional contacts—new insights for state-dependent properties. *Pure Appl. Geophys.* **143,** 283–302 (1994).
9. Ranjith, K. & Rice, J. R. Stability of quasi-static slip in a single degree of freedom elastic system with rate and state dependent friction. *J. Mech. Phys. Solids* **47,** 1207–1218 (1999).
10. Rice, J. R., Lapusta, N. & Ranjith, K. Rate and state dependent friction and the stability of sliding between elastically deformable solids. *J. Mech. Phys. Solids* **49,** 1865–1898 (2001).
11. Dieterich, J. H. Modeling of rock friction. 1. Experimental results and constitutive equations. *J. Geophys. Res.* **84** (B5), 2161–2168 (1979).
12. Ruina, A. Slip instability and state variable friction laws. *J. Geophys. Res.* **88** (B12), 10359–10370 (1983).

13. Griggs, D. Hydrolytic weakening of quartz and other silicates. *Geophys. J. R. Astron. Soc.* **14,** 19–31 (1967).
14. Scholz, C. H. & Engelder, J. T. The role of asperity indentation and ploughing in rock friction–I: Asperity creep and stick-slip. *Int. J. Rock Mech. Min. Sci. Geomech. Abstr.* **13,** 149–154 (1976).
15. Hirth, J. & Rice, J. On the thermodynamics of adsorption at interfaces as it influences decohesion. *Metall. Mater. Trans. A* **11,** 1501–1511 (1980).
16. Frye, K. M. & Marone, C. Effect of humidity on granular friction at room temperature. *J. Geophys. Res.* **107,** 2309, doi:10.1029/2001JB000654 (2002).
17. Michalske, T. A. & Fuller, E. R. Closure and repropagation of healed cracks in silicate glass. *J. Am. Ceram. Soc.* **68,** 586–590 (1985).
18. Stavrinidis, B. & Holloway, D. G. Crack healing in glass. *Phys. Chem. Glasses* **24,** 19–25 (1983).
19. Ben-David, O., Rubinstein, S. M. & Fineberg, J. Slip-stick and the evolution of frictional strength. *Nature* **463,** 76–79 (2010).
20. Bowden, F. P. & Tabor, D. *The Friction and Lubrication of Solids* Ch. I (Oxford University Press, 1958).
21. Weeks, J. D., Beeler, N. M. & Tullis, T. E. Frictional behavior: glass is like a rock. *Eos* **72,** (Fall Meeting Abs. Supp.) 457–458 (1991).
22. Kendall, K. *Molecular Adhesion and its Applications: The Sticky Universe.* (Springer, 2001).
23. Roche, A. *et al.* in *Ultra Clean Processing of Silicon Surfaces 2000* (eds Heyns, M., Mertens, P. & Meuris, M.) 76–77, 111–114 (Scitec, 2001).
24. Iler, R. K. *Chemistry of Silica—Solubility, Polymerization, Colloid and Surface Properties and Biochemistry* Ch. 1 (John Wiley & Sons, 1979).
25. Ploessl, A. & Krauter, G. Wafer direct bonding: tailoring adhesion between brittle materials. *Mater. Sci. Eng. Rep.* **25,** 1–88 (1999).
26. Thoms, B. D., Owens, M. S., Butler, J. E. & Spiro, C. Production and characterization of smooth, hydrogen-terminated diamond c(100). *Appl. Phys. Lett.* **65,** 2957–2959 (1994).
27. Oliver, W. C. & Pharr, G. M. An improved technique for determining hardness and elastic-modulus using load and displacement sensing indentation experiments. *J. Mater. Res.* **7,** 1564–1583 (1992).
28. Sader, J. E., Chon, J. W. M. & Mulvaney, P. Calibration of rectangular atomic force microscope cantilevers. *Rev. Sci. Instrum.* **70,** 3967–3969 (1999).
29. Li, Q., Kim, K. S. & Rydberg, A. Lateral force calibration of an atomic force microscope with a diamagnetic levitation spring system. *Rev. Sci. Instrum.* **77,** 065105 (2006).

Supplementary Information is linked to the online version of the paper at www.nature.com/nature.

Acknowledgements We thank M.O. Robbins, I. Szlufarska and Y. Liu for discussions. We acknowledge support from the National Science Foundation under awards EAR0810088 and EAR0810192.

Author Contributions Q.L. performed experiments and obtained the data, and analysed the data with input from all other authors. All four authors wrote this manuscript together. D.G. prepared some of the tips used for the experiments.

Author Information Reprints and permissions information is available at www.nature.com/reprints. The authors declare no competing financial interests. Readers are welcome to comment on the online version of this article at www.nature.com/nature. Correspondence and requests for materials should be addressed to R.W.C. (carpick@seas.upenn.edu).

METHODS

Friction force microscopy. Friction force microscopy was conducted using an RHK UHV350 AFM. A schematic of the setup of a friction force microscope is shown in Supplementary Fig. 1. The microscope consists of a sharp tip in contact with the surface of the sample. The tip is integrated with the end of a microfabricated cantilever that deforms in response to normal and lateral (friction) forces arising from the contacting interface. Deformation of the cantilever is measured with an optical system consisting of a laser and a quadrant photo detector. For frictional sliding, the back end of the cantilever is displaced relative to the sample along the indicated scan direction. Because of the extremely small tip radius, the lateral size of the contacting interface is usually a few to tens of nanometres, which provides an ideal single-asperity contact. During a friction experiment, the relative lateral displacement between the sample and the holder is increased at a constant rate and the resulting lateral force is measured while the normal load is maintained constant via an active feedback loop.

Normal and lateral force constants of the probes were calibrated using Sader's method[28] and a diamagnetic lateral force calibrator[29] respectively. All measurements were carried out in a sealed chamber with RH varied by bubbling pure dry nitrogen vapour from a liquid nitrogen dewar through water (or pure nitrogen, for measurements quoted at $<$1% RH). The system was equilibrated for at least 4 h after each humidity change. RH was monitored by a hygrometer (uncertainty $\pm$1.5% RH).

Sample preparation. The probes and substrate were processed by heating silicon probes (CSC37 Mikromasch) and Si(100) wafers in pure oxygen for 150 min and 300 min, respectively, to form oxides 100 nm and 400 nm thick (determined by ellipsometry), respectively. The substrates were cleaned with Piranha solution, rinsed with de-ionized water, dried under pure nitrogen flow, then rapidly inserted into the AFM. The substrates have a typical root-mean-square roughness of about 0.2 nm within 0.5 μm $\times$ 0.5 μm area as measured by an AFM.

The hydrogen-terminated diamond sample was grown by chemical vapour deposition (typical grain size $\sim$1 μm) and subsequently exposed to atomic hydrogen using an established method[26]. The graphite surface was prepared by freshly cleaving bulk highly ordered pyrolytic graphite.

SA-SHS experiments. A typical friction experiment is performed by first making contact between the tip and substrate, then sliding for an initial run-in distance (typically $\sim$1 mm, in successive 1-μm back-and-forth lateral displacements). Then, without breaking contact, a slide–hold–slide procedure was used in which the tip is slid for a prescribed distance (typically $\sim$400 nm), then held stationary for a time t_{hold}, and then lateral displacement is resumed. Constant normal load is imposed by a feedback loop. Four different hold times, in an alternating sequence of 0.1 s, 100 s, 1 s and 10 s, were used.

Two protocols are used as shown by the schematics in Supplementary Fig. 2. Supplementary Fig. 2a shows the positive lateral hold force protocol. The tip is slid for an initial distance (a[1], a[2]), then held stationary for a time t_{hold} without changing the lateral force (a[3]). Sliding is then reinitiated in the same direction by ramping up the lateral force (a[4]). Supplementary Fig. 2b shows the negative lateral hold force protocol. The tip is slid for an initial distance (b[1]), and then held stationary for a time t_{hold} without changing the lateral force (b[2]). Sliding is then reinitiated in the opposite direction by ramping up the lateral force (b[3], b[4]). The lateral force during the hold is 'positive' and usually very close to the steady-state friction value for the positive lateral hold force protocol, and is 'negative' and very close to the steady-state friction level for the negative lateral hold force protocol. The results shown in the main text are obtained using the positive hold force protocol; the results from the negative hold force protocol are given in Supplementary Figs 6 and 7 for comparison.